



Relationship between Cu₂ZnSnS₄ quasi donor-acceptor pair density and solar cell efficiency

Talia Gershon, Byungha Shin, Tayfun Gokmen, Siyuan Lu, Nestor Bojarczuk, and Supratik Guha

Citation: [Applied Physics Letters](#) **103**, 193903 (2013); doi: 10.1063/1.4829920

View online: <http://dx.doi.org/10.1063/1.4829920>

View Table of Contents: <http://scitation.aip.org/content/aip/journal/apl/103/19?ver=pdfcov>

Published by the [AIP Publishing](#)

Articles you may be interested in

[Improving the conversion efficiency of Cu₂ZnSnS₄ solar cell by low pressure sulfurization](#)

Appl. Phys. Lett. **104**, 141101 (2014); 10.1063/1.4870508

[The reversal of the laser-beam-induced-current contrast with varying illumination density in a Cu₂ZnSnSe₄ thin-film solar cell](#)

Appl. Phys. Lett. **103**, 242104 (2013); 10.1063/1.4844815

[Toward a high Cu₂ZnSnS₄ solar cell efficiency processed by spray pyrolysis method](#)

J. Renewable Sustainable Energy **5**, 053137 (2013); 10.1063/1.4825253

[Control of an interfacial MoSe₂ layer in Cu₂ZnSnSe₄ thin film solar cells: 8.9% power conversion efficiency with a TiN diffusion barrier](#)

Appl. Phys. Lett. **101**, 053903 (2012); 10.1063/1.4740276

[Admittance spectroscopy of Cu₂ZnSnS₄ based thin film solar cells](#)

Appl. Phys. Lett. **100**, 233504 (2012); 10.1063/1.4726042



Free online magazine

MULTIPHYSICS SIMULATION

[READ NOW ▶](#)



Relationship between $\text{Cu}_2\text{ZnSnS}_4$ quasi donor-acceptor pair density and solar cell efficiency

Talia Gershon, Byungha Shin, Tayfun Gokmen, Siyuan Lu, Nestor Bojarczuk, and Supratik Guha

IBM T. J. Watson Research Center, 1101 Kitchawan Rd., Yorktown Heights, New York 10598, USA

(Received 22 August 2013; accepted 27 October 2013; published online 7 November 2013)

We examined the 4 K photoluminescence spectra of over a dozen $\text{Cu}_2\text{ZnSnS}_4$ films and eight devices. We show that samples deficient in zinc show on average a higher quasi donor-acceptor pair (QDAP) density. However, the QDAP density in samples with the same metal composition also varies widely. Devices prepared with similar metal compositions show different open-circuit voltages and fill factors. These metrics are correlated with the concentration of QDAPs in the absorbers. One additional device with insufficient zinc showed the empirically observed low-efficiency expected for this composition. This sample also showed the highest quasi donor-acceptor pair density of all the devices measured. © 2013 AIP Publishing LLC. [<http://dx.doi.org/10.1063/1.4829920>]

$\text{Cu}_2\text{ZnSnS}_4$ (CZTS) is a promising photovoltaic absorber material with a complicated phase diagram and defect structure.^{1–5} Many studies, both experimental and theoretical, have highlighted the abundance of intrinsic defects in CZTS and the heavy compensation that results from the presence of both donors and acceptors.^{6–11} It has also been empirically observed that high-efficiency solar cells require a “zinc-rich” and “copper-poor” absorber although exactly what is achieved through this non-stoichiometry is unclear.^{1,4,5,12,13} There is still a lack of understanding regarding the inter-relatedness of point defects, starting metal compositions, and device efficiency in CZTS. Understanding the defect structure of CZTS, which factors influence defect distributions the most, and how these defects impact solar cell efficiency would help provide valuable insights for further advancing this technology.

One powerful tool for probing defects in semiconductors is low-temperature photoluminescence (PL).^{14–18} We carried out intensity-dependent photoluminescence measurements at 4 K on a variety of CZTS samples using a liquid helium cooled Janis-VP continuous flow cryostat equipped with a 532 nm pulsed laser (15 kHz) with a filter wheel controlling the incident power between $\sim 0.001 \text{ W/cm}^2$ and 0.668 W/cm^2 .

Samples of varying compositions were prepared according to previously-published methods.⁵ Briefly, thin films of CZTS (Cu/Sn ~ 1.72 – 1.87 , Zn/Sn variable, compositions measured via calibrated x-ray fluorescence (XRF)) were co-evaporated in the presence of sulfur onto pre-cleaned Mo-coated glass substrates held at 150°C . Samples were then annealed in a glove box on a hot plate at high temperature ($T > 550^\circ\text{C}$) with excess sulfur provided. Some samples were tested in completed devices. These underwent the following additional processing steps: a cyanide etch to remove residual Cu_2S if present, a 90–100 nm layer of CdS prepared by chemical bath deposition, a ZnO/ITO bilayer electrode, and a Ni/Al contact grid. Completed solar cell testing was performed under standard solar simulation, AM 1.5 G, 100 mW/cm^2 before PL characterization.

As discussed more extensively in a separate publication,¹⁸ intensity-dependent PL measurements at 4 K can be used to estimate the quasi donor-acceptor pair (QDAP)

defect density in CZTS, where the word “quasi” is used to indicate likely deviations from the classical model resulting from interacting defects, e.g., clustering.¹⁹ At low laser intensity, the PL spectrum of CZTS is comprised of a low-energy peak ($\sim 1.14 \text{ eV}$), which blue-shifts as the laser power increases. Above a threshold excitation intensity the spectrum develops a higher-energy shoulder ($\sim 1.4 \text{ eV}$), and the low-energy peak simultaneously saturates in height and red-shifts.

The blue-shifting low-energy peak represents emission through localized quasi donor and acceptor states and is discussed further below. The high-energy shoulder represents recombination involving at least one set of extended states, e.g., a band,¹⁸ and appears only after the localized states have been fully saturated. The fundamental difference in recombination mechanism between the low-energy peak and the high-energy shoulder is highlighted by the carrier lifetimes at 4 K; while the lifetime associated with the 1.2 eV peak is $\sim 10 \mu\text{s}$, the lifetime associated with the 1.4 eV peak is $\sim 2 \text{ ns}$.¹⁸ Thus, at 4 K the 1.2 eV emission must involve carriers in localized states while the 1.4 eV emission must involve states that are delocalized. A further discussion of these peaks and the methods used to identify them are presented in a separate publication.¹⁸ The saturation of the low-energy peak height and peak position ($\langle E_g \rangle$) as well as the presence of a high-energy shoulder with much shorter lifetime indicate that the lower-energy blue-shifting peak must be caused by QDAP defects.

The blue-shift of the QDAP peak stems from the Coulombic interaction between neutral defects, i.e., donors that are populated with an electron and acceptors that are populated with a hole. The density of neutral defects (and therefore their proximity to each other) is proportional to the excitation intensity. More closely spaced neutral defects experience stronger Coulombic interactions, and the release of the Coulombic interaction energy results in an increase in the energy of the emitted photon. This phenomenon is described by Eq. (1), where E is the luminescence energy, E_g is the band gap energy, E_D is the average quasi-donor ionization energy, E_A is the average quasi-acceptor ionization

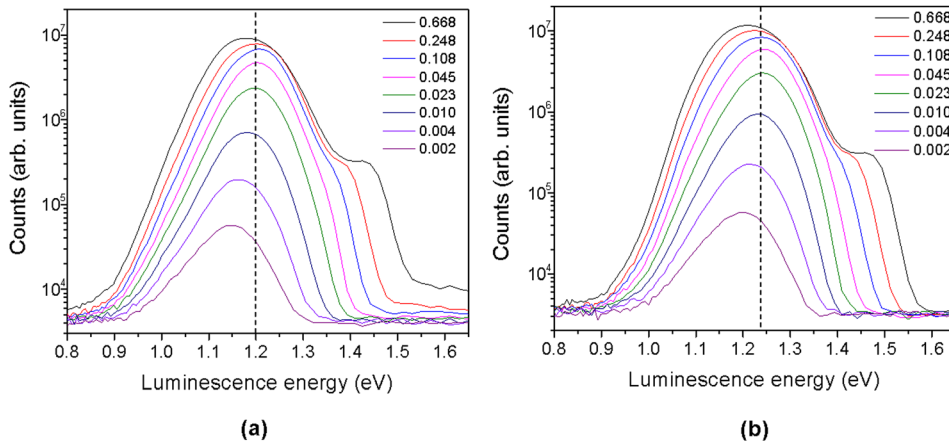


FIG. 1. Intensity-dependent PL measurements of CZTS films with different compositions (laser power indicated in the legend, W/cm^2). (a) $\text{Cu}/\text{Sn} = 1.75$, $\text{Zn}/\text{Sn} = 1.24$; (b) $\text{Cu}/\text{Sn} = 1.72$, $\text{Zn}/\text{Sn} = 1.0$. The dashed line guides the eye to the saturated QDAP peak position.

energy, q is the elementary charge, ϵ is the dielectric constant, and r is the average spacing between neutral quasi donors and acceptors.¹⁴ We note that the abundance of QDAP defects results in a distribution of energy levels around the average values E_D and E_A , giving rise to wide PL peaks. E_g , E_A , and E_D are all approximately constants

$$E = E_g - E_D - E_A + \frac{q^2}{4\pi\epsilon r}. \quad (1)$$

The blue-shift saturates when all ionized QDAPs become neutral. If we assume that at the lowest laser power the energy of interaction between neutral defects is small, then the energy of the shift between the initial and saturated QDAP peak positions corresponds to the Coulombic interaction energy in Eq. (1). From this we can estimate the average spacing between the defects.

A typical intensity-dependent spectrum observed for CZTS films and devices is shown in Figure 1(a). In this sample ($\text{Cu}/\text{Sn} = 1.75$, $\text{Zn}/\text{Sn} = 1.25$), the energy at which the QDAP peak saturates is 1.20 eV ($0.05 \text{ W}/\text{cm}^2$). By contrast, Figure 1(b) shows the PL spectra from a different sample ($\text{Cu}/\text{Sn} = 1.72$, $\text{Zn}/\text{Sn} = 1.0$) wherein the QDAP peak saturates at 1.24 eV ($0.05 \text{ W}/\text{cm}^2$). We assume that the *types* of defects contributing to the PL in all of the samples we measured are the same. This is because of the similarity in spectral shape and the fact that the peak at the lowest laser power is centered at approximately the same energy ($1.14 \pm 0.01 \text{ eV}$) for all samples (data not shown). A higher-energy saturated QDAP peak position therefore represents a stronger Coulombic interaction between defects, a closer average defect spacing, and thus a higher QDAP density.

Figure 2 presents the saturated QDAP peak position of 16 samples of varying zinc content, where the Cu/Sn ratio remains similar (between 1.72 and 1.87). From Figure 2 it can be seen that on average as the zinc content decreases the QDAP peak shifts to higher energy, implying an increased QDAP density, where the defect spacing r is related to the defect density N_D by $r = (4\pi N_D/3)^{-1/3}$.¹⁹ We note that there is significant scatter in the QDAP peak position even for a constant Cu/Zn ratio. Thus, other factors must also contribute to the defect distribution in CZTS. Variations in composition are also expected to produce secondary phases, e.g., ZnS , SnS , Cu_2S , Cu_2SnS_3 , and others.^{1,2,13,21} However, we do not observe additional PL peaks associated with these

other materials, likely due to the differences in the optical properties between CZTS and its secondary phases (e.g., ZnS has a wide band gap, SnS has an indirect band gap, etc.) and/or the fact that this method probes only the $\sim 100 \text{ nm}$ of material closest to the surface. Thus Figure 2 represents the changes to the optical properties of the CZTS component of whatever mixed-phase material was formed.

We examined the low-temperature PL of 7 CZTS devices (no anti-reflection layer) of similar composition ($\text{Cu}/\text{Sn} = 1.75\text{--}1.87$, $\text{Zn}/\text{Sn} = 1.11\text{--}1.23$) and one sample considered to be “low-zinc” ($\text{Cu}/\text{Sn} = 1.75$, $\text{Zn}/\text{Sn} = 1.04$). Despite 7 of the samples having similar metal compositions, these displayed wide variations in open-circuit voltage (V_{oc}) values and fill factor (FF) values. The samples also showed variations in saturated QDAP peak position. When plotted together (Figure 3), it is clear that these parameters are strongly correlated with the saturated QDAP peak position. This again indicates that the metal ratios are not the only parameters contributing to defect distributions and thus device efficiency. The “low-zinc” device had both the worst performance and the highest saturated QDAP peak position, which is likely related to the empirical observation that “zinc-rich” and “copper-poor” samples result in better device performance.

The average spacing between donors and acceptors was estimated according to Eq. (1) and previously determined values of the CZTS dielectric constant.²⁰ A saturated QDAP

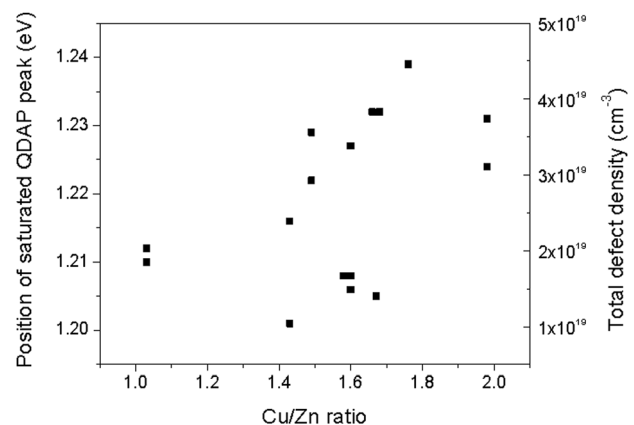


FIG. 2. Right axis: relationship between Cu/Zn ratio and the saturated QDAP peak position (with $\text{Cu}/\text{Sn} = 1.72\text{--}1.87$). The peak position at the lowest laser intensity is $1.14 \pm 0.01 \text{ eV}$. Left axis: calculated total defect density based on PL peak shift.

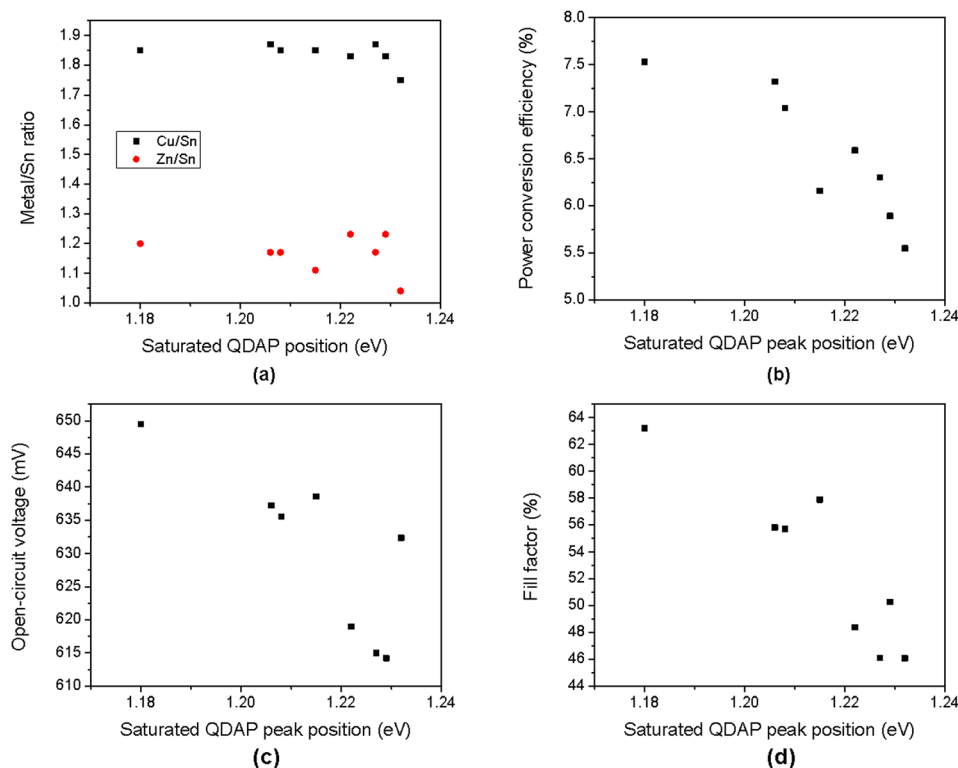


FIG. 3. (a) Compositions of 7 “similar” CZTS films and one “low-zinc” film (as determined via calibrated XRF measurements), displayed as a function of the saturated QDAP peak position. (b)–(d) Power conversion efficiencies, V_{oc} values, and FF values, respectively, of devices made with these absorbers as a function of QDAP peak position.

peak position of ~ 1.2 eV corresponds to a quasi donor-acceptor spacing of roughly 3.52 nm (and hence a total defect density of $N_t = 1.1 \times 10^{19} \text{ cm}^{-3}$) while a saturated peak position of ~ 1.24 eV corresponds to a QDAP spacing of roughly 2.17 nm ($N_t = 4.7 \times 10^{19} \text{ cm}^{-3}$). Higher-energy saturated QDAP peaks therefore correspond to closer spacing between donors and acceptors and heavier compensation. Large defect densities and heavy compensation are expected to reduce both the V_{oc} , e.g., due to the formation of tail states,²² and the FF, inasmuch as defects may participate in trapping and recombination processes.^{15,23–25}

In conclusion, low-temperature photoluminescence measurements can be used to estimate the density of quasi donors and acceptors in CZTS films. We show that the total defect density is influenced by the zinc content of the absorber. Additionally, for a given composition, there is significant scatter in the concentration of QDAP defects, thus indicating other contributing factors besides the metal ratios. We also show that the saturated QDAP peak position (or equivalently the total defect density) is a better indicator of device efficiency than the starting metal ratios alone.

¹D. B. Mitzi, O. Gunawan, T. K. Todorov, K. Wang, and S. Guha, *Sol. Energy Mater. Sol. Cells* **95**, 1421 (2011).

²S. Siebentritt and S. Schorr, *Prog. Photovoltaics* **20**, 512 (2012).

³I. Repins, N. Vora, C. Beall, S.-H. Wei, Y. Yan, M. Romero, G. Teeter, H. Du, B. To, M. Young, and R. Noufi, *Kesterites and Chalcopyrites: A Comparison of Close Cousins* (U.S. Department of Energy, 2011).

⁴T. K. Todorov, J. Tang, S. Bag, O. Gunawan, T. Gokmen, Y. Zhu, and D. B. Mitzi, *Adv. Energy Mater.* **3**, 34 (2013).

⁵B. Shin, O. Gunawan, Y. Zhu, N. A. Bojarczuk, S. J. Chey, and S. Guha, *Prog. Photovoltaics* **21**, 72 (2013).

⁶A. Walsh, S. Chen, X. G. Gong, and S.-H. Wei, *AIP Conf. Proc.* **1399**, 63 (2011).

⁷S. Chen, X. G. Gong, A. Walsh, and S.-H. Wei, *Appl. Phys. Lett.* **96**, 021902 (2010).

⁸S. Chen, J.-H. Yang, X. G. Gong, A. Walsh, and S.-H. Wei, *Phys. Rev. B* **81**, 245204 (2010).

⁹S. Chen, A. Walsh, X.-G. Gong, and S.-H. Wei, *Adv. Mater.* **25**(11), 1522 (2013).

¹⁰S. Schorr, *Sol. Energy Mater. Sol. Cells* **95**(6), 1482 (2011).

¹¹T. Washio, H. Nozaki, T. Fukano, T. Motohiro, K. Jimbo, and H. Katagiri, *J. Appl. Phys.* **110**, 074511 (2011).

¹²T. Unold, S. Kretzschmar, J. Just, O. Zander, B. Schubert, B. Marsen, and H.-W. Schock, “Correlation between composition and photovoltaic properties of $\text{Cu}_2\text{ZnSnS}_4$ thin film solar cells,” in *Photovoltaic Specialists Conference* (IEEE, 2011).

¹³J. J. Scragg, “Studies of $\text{Cu}_2\text{ZnSnS}_4$ films prepared by sulfurisation of electrodeposited precursors,” Ph.D. Thesis (University of Bath, 2010).

¹⁴J. I. Pankove, *Optical Processes in Semiconductors* (Dover Publications, Inc., New York, 1971).

¹⁵P. Y. Yu and M. Cardona, *Fundamentals of Semiconductors* (Springer-Verlag, Heidelberg, 2010).

¹⁶P. W. Yu, *J. Appl. Phys.* **48**, 5043 (1977).

¹⁷S. Zott, K. Leo, M. Ruckh, and H.-W. Schock, *J. Appl. Phys.* **82**, 356 (1997).

¹⁸T. Gershon, B. Shin, N. Bojarczuk, T. Gokmen, S. Lu, and S. Guha, *J. Appl. Phys.* **114**, 154905 (2013).

¹⁹B. I. Shklovskii and A. L. Efros, *Electronic Properties of Doped Semiconductors* (Springer-Verlag, Berlin/Heidelberg, 1984).

²⁰C. Persson, *J. Appl. Phys.* **107**, 053710 (2010).

²¹C. Leidholm, C. Hotz, A. Breeze, C. Sunderland, W. Ki, and D. Zehnder, Final report: Sintered CZTS nanoparticle solar cells on metal foil, U.S. Department of Energy, 2012.

²²T. Gokmen, O. Gunawan, T. K. Todorov, and D. B. Mitzi, *Appl. Phys. Lett.* **103**, 103506 (2013).

²³D. Macdonald and A. Cuevas, *Prog. Photovoltaics* **8**, 363 (2000).

²⁴I. Repins, M. A. Contreras, B. Egaas, C. DeHart, J. Scharf, C. L. Perkins, B. To, and R. Noufi, *Prog. Photovoltaics* **16**, 235 (2008).

²⁵A. J. Lofthfeld, M. R. Melloch, J. C. P. Chang, and E. S. Harmon, *Appl. Phys. Lett.* **69**, 1465 (1996).